Simulating Terahertz Plasma Oscillations in Transistors

Ashwin Tunga
Electrical and Computer Engineering
University of Illinois Urbana-Champaign
Urbana, IL, 61801, USA
tunga2@illinois.edu

Michael Shur
Electrical, Computer, and Systems Engineering
Rensselaer Polytechnic Institute
Troy, NY, 12180, USA
shur@rpi.edu

Matt Grupen
AFRL Sensors Directorate, WPAFB
OH, 45433, USA
matthew.grupen@us.af.mil

David Hill
SRI International
201 Washington Rd,
Princeton, NJ, 08540, USA
david.hill@sri.com

Shaloo Rakheja
Electrical and Computer Engineering
University of Illinois Urbana-Champaign
Urbana, IL, 61801, USA
rakheja@illinois.edu

***Abstract*—Terahertz plasma oscillations in GaN HEMTs are simulated in a TCAD environment using the Fermi kinetics transport model. Parallels are drawn between the Boltzmann transport equation and the shallow water dynamics used in previous studies to explain the oscillations. The necessary simulation conditions needed to observe the oscillations in a TCAD environment are described. Further discussion on the significance of the average momentum relaxation time and the rationale for choosing its value are presented. Transient simulations of THz oscillations are demonstrated when the gate voltage is perturbed at the quiescent point. A physical theory of plasma oscillations is proposed by analyzing the oscillations of the channel electron concentration, electron temperature and electric field. The electron temperature and electric field profiles are observed to be out of phase with each other, alluding to the fact that the energy is exchanged back and forth between the hot electrons and the EM fields, leading to the excitation of plasma oscillations.**

***Index Terms*—Plasma wave transistors, Dyakonov–Shur instability, GaN HEMT, Fermi kinetics transport**

I. Introduction

The theoretical groundwork for plasma wave transistors was laid by Dyakonov and Shur [1], who observed that the Boltzmann transport equation (BTE) in the relaxation time approximation and under near ballistic conditions, resembles the Euler equation from shallow water hydrodynamics. They proposed that the channel electrons in a ballistic field effect transistor (FET) can behave like a viscous fluid. Their work demonstrated that the reduced equation set describing the electron flow exhibits numerical instability in a ballistic FET when subjected to asymmetric boundary conditions under a certain DC bias. The instability, termed the Dyakonov–Shur instability, is the result of the reflection of the plasma waves at the device boundaries, and leads to the spontaneous generation of plasma waves in the THz range. Subsequently, THz emission was experimentally demonstrated [2] in a 60 nm InGaAs HEMT at 4.2 K and the results were interpreted using the Dyakonov-Shur instability of the plasma waves. Additionally, THz detection [3] was demonstrated in GaAs HEMTs. This paper shows that the plasma wave generation can be simulated in a TCAD environment, contingent on the solver's ability to simulate coupled full-wave electromagnetics (EM) and near-ballistic hot electron transport. This paper sheds light on the necessary simulation capabilities, demonstrates simulated plasma oscillations in a test transistor structure, and proposes a physical theory of the origin of the plasma waves. Our results demonstrate a new type of plasmonic instability that occurs in the boundary drain channel edge region.

The transistor structure simulated in this work is an AlGaN/GaN HEMT. AlGaN/GaN HEMTs have demonstrated superior performance as high power switching transistors [4], RF transistors with record power [5], and, more recently, as TeraFETs for terahertz (THz) sensing applications and 6G communications [6], including detectors [7] and even emitters [8] of sub-THz and THz radiation.

This work was supported by AFOSR Grant No. LRIR 24RYCOR009, DARPA Agreement No. HR00112390072, and NSF Grant No. ECCS-2237663.

II. Overview of Fermi kinetics transport

In order to accurately capture the interaction between the electromagnetic fields and the charge carriers when simulating semiconductor devices in the THz operating range, it is essential to couple the full-wave EM with the charge transport. A full-wave EM simulation involves solving the Maxwell's equations:

$$\begin{aligned} \nabla \cdot \epsilon \mathbf{E} &= \rho \qquad & \nabla \cdot \mathbf{B} &= 0 \\ \nabla \times \mathbf{E} &= -\frac{\partial \mathbf{B}}{\partial t} \qquad & \nabla \times \mathbf{B} &= \mu_0 \left(\mathbf{J} + \frac{\partial \epsilon \mathbf{E}}{\partial t} \right). \end{aligned} \tag{1}$$

Furthermore, the Boltzmann transport equation (BTE) accounts for the hot electron dynamics. The first moment of the BTE under the relaxation time approximation is given by

$$\mathbf{J} + \bar{\tau} \frac{\mathrm{d}\mathbf{J}}{\mathrm{d}t} = -\frac{q}{4\pi^3} \int \tau_{\mathbf{k}} \boldsymbol{v} \left(q\mathbf{E} \cdot \frac{1}{\hbar} \nabla_{\mathbf{k}} f_0 - \boldsymbol{v} \cdot \nabla f_0 \right) \mathrm{d}\mathbf{k}, \tag{2}$$

where $\mathbf{J}$ is the electron current density, $\boldsymbol{v}$ is the group velocity, $\mathbf{E}$ is the external applied electric field, f_0 is the even part of the distribution function, $\tau_{\mathbf{k}}$ is the momentum relaxation time, and $\bar{\tau}$ is the average momentum relaxation time. It is important to note that the term $\bar{\tau}\frac{\mathrm{d}\mathbf{J}}{\mathrm{d}t}$ could be analogous to the viscosity of the electron fluid in the analysis presented in [1]. This further alludes to the point that the BTE resembles the shallow water dynamics, and that a TCAD BTE solver can simulate plasma oscillations. However, a clear physical connection between TCAD and shallow water dynamics will be investigated in future work.

In this work, the aforementioned set of equations are solved in a unique TCAD environment called the Fermi kinetics transport (FKT) solver, developed at the Air Force Research Laboratory. FKT is a deterministic Boltzmann transport solver that employs the method of moments to compute the electron and the energy fluxes. The electron flux, obtained from the first moment of the BTE, is given by (2). The electron kinetic energy flux, obtained from the third moment, is given by

$$\mathbf{K} + \bar{\tau}\frac{\mathbf{K}}{dt} = \frac{1}{4\pi^3}\int E\boldsymbol{v}\left[\frac{q\tau_{\mathbf{k}}}{\hbar}\mathbf{E}\cdot\nabla_k f - \tau_{\mathbf{k}}\boldsymbol{v}\cdot\nabla f\right]\mathrm{dk}. \quad (3)$$

The key departure of FKT from conventional BTE solvers is in the treatment of the electronic heat flow. FKT treats the electronic heat flow using the heat capacity of an ideal Fermi gas [9], given by

$$H = \int_{T_i}^{T_f} C_{el}\mathrm{d}T = \int_{T_i}^{T_f} C_{el}\left[\frac{1}{4\pi^3}\int_{\mathbf{k}}(E-F)\frac{\mathrm{d}f}{\mathrm{d}T}\mathrm{d}\mathbf{k}\right]\mathrm{d}T, \quad (4)$$

where H is the energy required to heat a Fermi gas from an initial temperature T_i to a final temperature T_f. This is unlike the conventional Boltzmann solvers that utilize the Fourier's law to model electronic heat flow. This alternative treatment has enabled FKT to exhibit better numerical stability and convergence behavior [10]. Furthermore, FKT can incorporate the electronic bandstructure, the essential electron scattering mechanisms and, crucially, the full-wave electromagnetics (EM) [11]. To incorporate the full-wave EM, the FKT charge transport model is coupled self-consistently with Maxwell's vector field equations. Maxwell's equations are discretized with Delaunay/Voronoi surface integration (DVSI), and are implemented with fully implicit backward Euler time stepping.

III. Simulation Setup

The structure of the GaN HEMT is based on the device fabricated and characterized by Palacios et al. [12]. The simulated device structure and the mesh used for the simulations are shown in Fig. 1(a) and (b), respectively. All the metals are considered to be perfect electrical conductors (PEC). The source and drain contacts are treated as ohmic contacts, while the gate is treated as a Schottky contact with a barrier height of 1.2 eV. For full-wave simulations, a voltage boundary condition (BC) is necessary to enable EM energy to enter and exit the simulation domain when a voltage source is applied. A voltage BC is defined at the source, drain, and gate terminals. Further details on the implementation of the voltage BC can be found in [11]. The lattice temperature is assumed to be at 300 K at the backplane of the SiC substrate. Hole transport was not considered in these simulations.

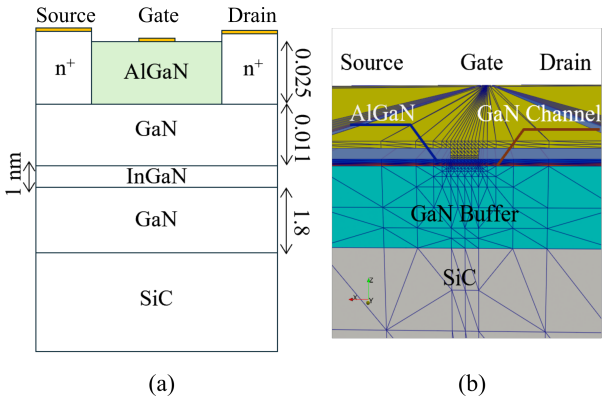

Fig. 1. (a) Schematic of the GaN HEMT structure. All the dimensions are in μm, unless mentioned otherwise. (b) The mesh of the device used for the simulations.

As highlighted in [1], to observe plasma waves in HEMTs, the charge transport has to be ballistic in nature with minimal phonon and impurity scattering, where the momentum relaxation time exceeds the electron transit time through the pinched-off region of the channel when biased in saturation. To create these conditions in the simulated structure, we chose 1 ps for the average momentum relaxation lifetime $\bar{\tau}$ in the first moment of the Boltzmann equation (2). Although rapid electron-phonon scattering in the GaN material system results in a much smaller, sub-picosecond value for $\bar{\tau}$, the larger value allows the simulation to capture the plasma oscillation effect in this HEMT device geometry at room temperature.

IV. Discussion

The FKT DC simulations were compared with the experimental measurements from [12]. Figure 2 shows good agreement over a wide bias range. When the device is biased

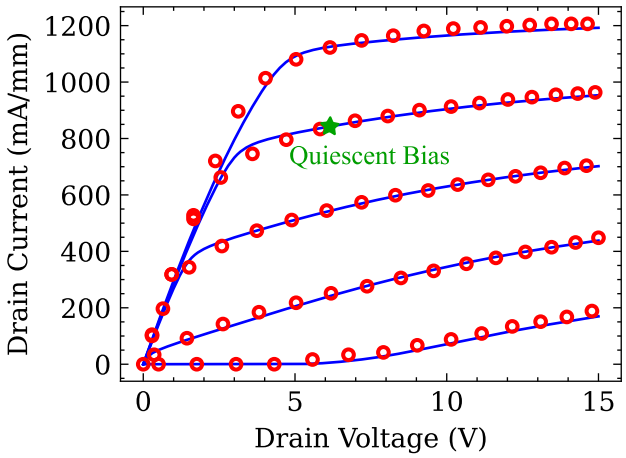

Fig. 2. DC output characteristics. V_{GS} varies from 1 V to -3 V. The quiescent bias is $V_{\mathrm{DS}} = 6$ V and $V_{\mathrm{GS}} = 0$ V, as indicated. Symbols represent the experimental measurement and the lines represent the simulated results.

at the quiescent bias voltage indicated in Fig. 2, where the hot electron mean free path is comparable to the gate length, then a perturbation of the channel by a Gaussian voltage pulse on the gate terminal can induce THz oscillations in the drain current long after the perturbation has dissipated. This is shown in Fig. 3; the inset shows the voltage perturbation at the gate.

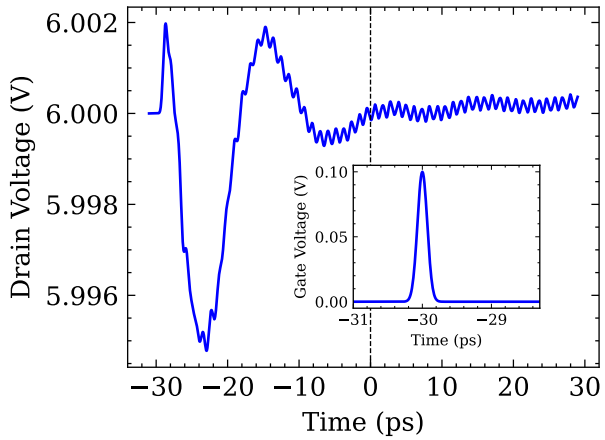

Fig. 3. THz drain voltage oscillations resulting from oscillating drain current and 50 Ω load resistance. Inset: Gaussian voltage pulse excitation at the gate.

Electron density dynamics may offer insights into the THz oscillations. As electron densities along the channel vary by orders of magnitude, Figure 4 shows the relative variation of the electron density with respect to the initial density at the corresponding channel location. When the applied voltage causes the channel to pinch off under the drain side of the gate, a low density of near ballistic hot electrons cross the pinch off region and collide with a high density of colder electrons in the drain access region. As the heat capacity of the degenerate electrons is relatively small, it may be that the hot electrons cannot transfer their heat to the cold dense electrons. Owing to their near-ballistic nature, the hot electrons also cannot transfer their energy to lattice phonons. Thus, it may be that the hot electrons must transfer their energy back to the EM fields by reversing their direction. The reflected electrons then encounter the cold electrons in the source access region, and the process repeats. The resulting adiabatic exchange of energy between the hot electrons and the fields may be one possible interpretation of the THz oscillations. Figures 5 and 6 show oscillations of the electron temperature and the electric field, respectively, from their DC values along the channel with time. The key point to note is that at any one of the time instants, the peak of the electron temperature occurs at the same location in the channel as the trough of the electric field, and vice versa. That is, the electron temperature and the electric field profiles are out of phase with each other. This suggests that hot electrons exchanging energy back and forth with EM fields might be the underlying source of the plasma oscillations. Continued research will further investigate this possibility through variations in device geometry, quiescent bias, and other simulations conditions.

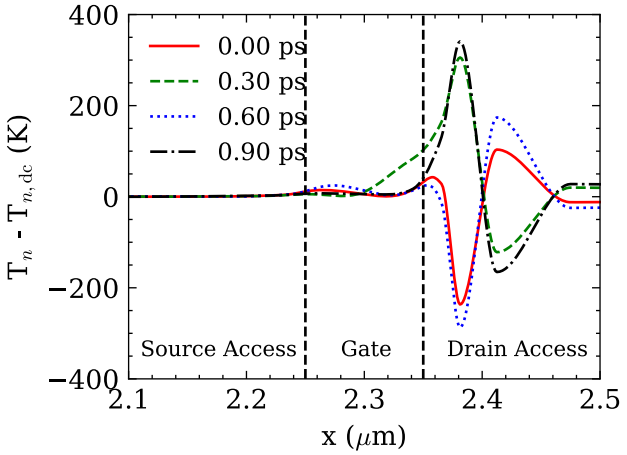

Fig. 5. Oscillation of the electron temperature (T_n) from its DC value with time, along the channel at the AlGaN/GaN interface. Link to animation of the figure, showing the channel electron temperature oscillations overlaid with the electric field oscillations.

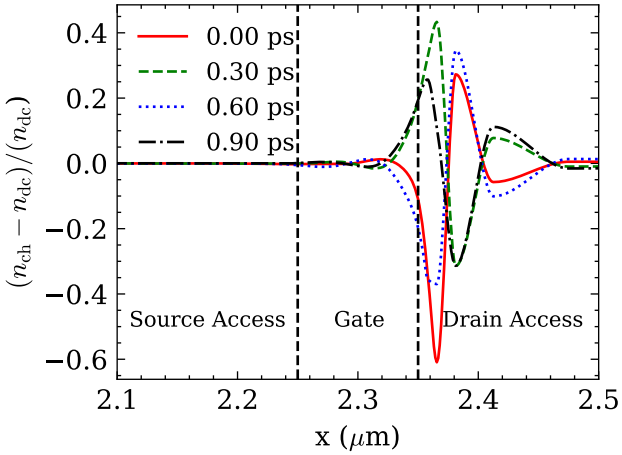

Fig. 4. Oscillation of the relative deviation of the electron concentration with time, along the channel at the AlGaN/GaN interface. Link to animation of the figure, showing the channel electron oscillations.

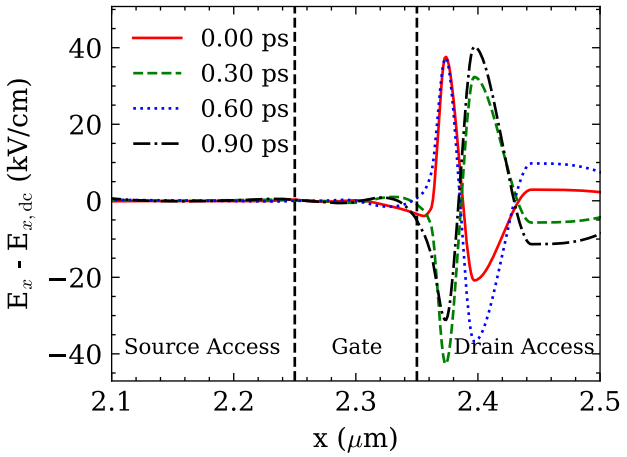

Fig. 6. Oscillation of the electric field (E_x) from its DC value with time, along the channel at the AlGaN/GaN interface. Link to animation of the figure, showing the channel electric field oscillations overlaid with the electron temperature oscillations.

V. Conclusion

In this paper, we utilize a TCAD solver to simulate plasma oscillations in a transistor. We identify the similarities of the Boltzmann equation with the shallow water dynamics of the electron fluid that was used to explain the plasma oscillations in previous works. Our work highlights the significance of a coupled EM and hot electron transport solver to simulate these oscillations in TCAD environment. Using the simulation results, we propose a physical theory of plasma oscillations based on near ballistic hot electrons interacting with lower heat capacity degenerate electrons, further advancing our understanding of these phenomena in semiconductor devices.

Appendix

As highlighted in Sec. II, the electron flux density obtained from the BTE is given by (2) and the term $\bar{\tau}\frac{\mathrm{d}\mathbf{J}}{\mathrm{d}t}$ could be analogous to the viscosity of the electron fluid. The average momentum relaxation time, $\bar{\tau}$, can be calculated using the following expression,

$$\bar{\tau} = \frac{\int_E \left[\int_{\mathbf{k}} v_x^2 \tau_{\mathbf{k}} \rho_{\mathbf{k}} \mathrm{d}\mathbf{k}\right] qE_x \frac{\mathrm{d}f}{\mathrm{d}E} \mathrm{d}E}{\int_E \left[\int_{\mathbf{k}} v_x^2 \rho_{\mathbf{k}} \mathrm{d}\mathbf{k}\right] qE_x \frac{\mathrm{d}f}{\mathrm{d}E} \mathrm{d}E}, \tag{5}$$

where $\rho_{\mathbf{k}}$ is the density of states, v_x is the drift velocity and E_x is the applied electric field. Figure 7 shows the time evolution of $\bar{\tau}$ in GaN when an electric field is applied at $t = 0$. As can be seen, $\bar{\tau}$ in a material is dependent on the electric field and evolves with time, and is generally sub-picosecond in GaN. As mentioned in Sec. IV, to observe plasma waves in HEMTS, the charge transport has to be ballistic in nature, where the momentum relaxation time exceeds the electron transit time. While this can be achieved by scaling the gate length of the device, it comes at the cost of the degradation of the electrostatics and the DC characteristics of the device. Figure 8 shows that as the gate length is scaled $10\times$, the device faces difficulty in turning off. This can be attributed to the poor gate control of the channel as the gate length scales. This requires redesigning the gate stack.

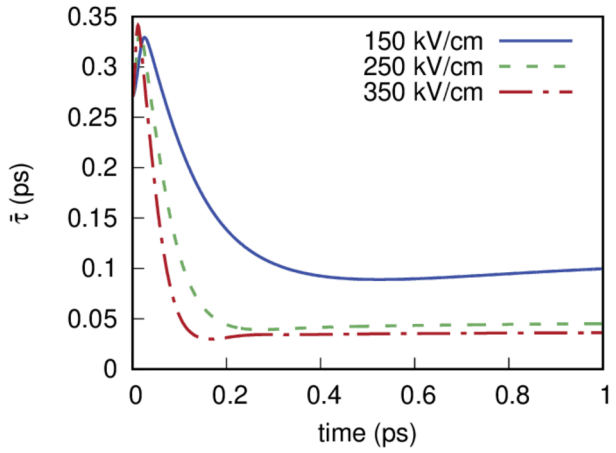

Fig. 7. Time evolution of the average momentum relaxation ($\bar{\tau}$) in bulk GaN with varying electric field, when an electric field is applied at $t = 0$.

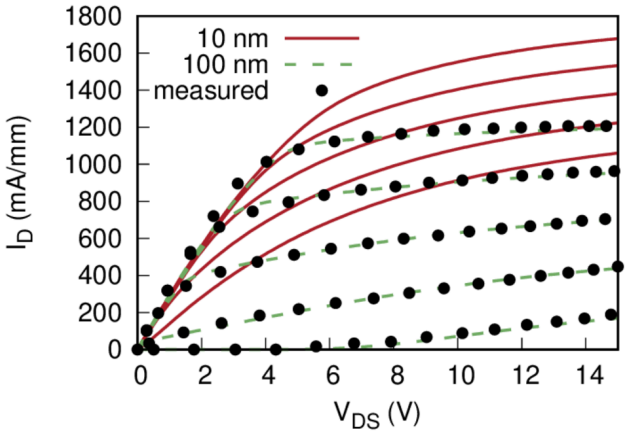

Fig. 8. The DC I_{D}-V_{DS} characteristics as the gate length is scaled. The dots represent the measured values of a 100 nm gate length device [12], and the lines represent the simulated results.

Distribution Statement

Approved for public release; distribution is unlimited.

References

[1] M. Dyakonov and M. Shur, "Shallow water analogy for a ballistic field effect transistor: New mechanism of plasma wave generation by dc current," *Physical Review Letters*, vol. 71, pp. 2465–2468, Oct. 1993.

[2] W. Knap, J. Lusakowski, T. Parenty, S. Bollaert, A. Cappy, V. V. Popov, and M. S. Shur, "Terahertz emission by plasma waves in 60 nm gate high electron mobility transistors," *Applied Physics Letters*, vol. 84, pp. 2331–2333, Mar. 2004.

[3] J.-Q. Lu, M. Shur, J. Hesler, L. Sun, and R. Weikle, "Terahertz detector utilizing two-dimensional electronic fluid," *IEEE Electron Device Letters*, vol. 19, pp. 373–375, Oct. 1998.

[4] M. Shur, X. Liu, and T. Ytterdal, "Switching characteristics of gan power transistors," *ECS Transactions*, vol. 112, no. 2, p. 45, 2023.

[5] W. Li, B. Romanczyk, M. Guidry, E. Akso, N. Hatui, C. Wurm, W. Liu, P. Shrestha, H. Collins, C. Clymore, *et al.*, "Record rf power performance at 94 ghz from millimeter-wave n-polar gan-on-sapphire deep-recess hemts," *IEEE Transactions on Electron Devices*, vol. 70, no. 4, pp. 2075–2080, 2023.

[6] N. Akter, N. Pala, W. Knap, and M. Shur, "THz plasma field effect transistor detectors," *Fundamentals of Terahertz Devices and Applications*, pp. 285–322, 2021.

[7] M. Bauer, A. Lisauskas, S. Boppel, M. Mundt, V. Krozer, H. G. Roskos, S. Chevtchenko, J. Würfl, W. Heinrich, and G. Tränkle, "Bow-tie-antenna-coupled terahertz detectors using AlGaN/GaN field-effect transistors with 0.25 micrometer gate length," in *2013 European Microwave Integrated Circuit Conference*, pp. 212–215, IEEE, 2013.

[8] G. Cywiński, K. Szkudlarek, I. Yahniuk, S. Yatsunenko, M. Siekacz, C. Skierbiszewski, W. Knap, D. B. But, D. Coquillat, and N. Dyakonova, "Gan/algan based transistors for terahertz emitters and detectors," in *2016 21st International Conference on Microwave, Radar and Wireless Communications (MIKON)*, pp. 1–4, IEEE, 2016.

[9] M. Grupen, "An alternative treatment of heat flow for charge transport in semiconductor devices," *Journal of Applied Physics*, vol. 106, p. 123702, Dec. 2009.

[10] A. Tunga, K. Li, E. White, N. C. Miller, M. Grupen, J. D. Albrecht, and S. Rakheja, "A comparison of a commercial hydrodynamics TCAD solver and Fermi kinetics transport convergence for GaN HEMTs," *Journal of Applied Physics*, vol. 132, p. 225702, Dec. 2022.

[11] M. Grupen, "Three-Dimensional Full-Wave Electromagnetics and Nonlinear Hot Electron Transport With Electronic Band Structure for High-Speed Semiconductor Device Simulation," *IEEE Transactions on Microwave Theory and Techniques*, vol. 62, pp. 2868–2877, Dec. 2014.

[12] T. Palacios, C.-S. Suh, A. Chakraborty, S. Keller, S. DenBaars, and U. Mishra, "High-performance E-mode AlGaN/GaN HEMTs," *IEEE Electron Device Letters*, vol. 27, pp. 428–430, June 2006.